Published in final edited form as:
J Immunol. 2014 July 15; 193(2): 529–539. doi:10.4049/jimmunol.1303247.

B Cells Regulate CD4+ T cell Responses to Papain Following BCR-Independent Papain Uptake

Daniel F. Dwyer[*], **Matthew C. Woodruff**[†], **Michael C. Carroll**[†], **K. Frank Austen**[*], and **Michael F. Gurish**[*]

[*]Division of Rheumatology, Immunology and Allergy, and Department of Medicine, Brigham and Women's Hospital, Harvard Medical School, Boston, MA

[†]Program in Cellular and Molecular Medicine, Boston Children's Hospital, Boston, MA 02115

Abstract

Papain, a cysteine protease allergen with inherent adjuvant activity, induces potent IL4 expression by T cells in the popliteal lymph nodes (PLN) of mice following footpad immunization. Here we identify a novel, non-BCR mediated capacity for B cells to rapidly bind and internalize papain. B cells subsequently regulate the adaptive immune response by enhancing Inducible T cell Costimulator (ICOS) expression on $CD4^+$ T cells and amplifying Th2 and T follicular helper induction. Antibody blockade of ICOS ligand, expressed by PLN B cells but not DC at the peak of the response, inhibits IL-4 responses in WT but not B cell-deficient mice. Thus, B cells play a critical role in amplifying adjuvant-dependent Th2 polarization following non-canonical acquisition and internalization of the cysteine protease papain.

Introduction

Allergens are a broad class of otherwise innocuous Ags capable of inducing vigorous Th2 responses. Allergens commonly provide adjuvant signals that direct innate and adaptive immune responses against associated proteins. Several common allergens, including grass pollen and house dust mite Ag, contain cysteine protease elements (1, 2), and these elements provide adjuvant effects (3). Infection with parasitic helminths also induces a host Th2 response that assists in parasite clearance (4), and helminth-secreted cysteine proteases play important roles in helminthic life cycles (5). The cysteine protease papain shares structural similarity with proteases found in both helminths (6) and allergens (7) and when injected into the mouse footpad induces a potent Th2 response in the popliteal lymph nodes (PLN) (8). Although an initial study failed to show a role for dendritic cells (DC) in Th2 polarization following papain immunization (9), subsequent studies established a central DC role in directing this response (10–13). However, the seminal finding that Th2 polarization is impaired in mice with MHC-II expression restricted to $CD11c^+$ cells (9) remains unresolved, indicating the need for a MHC-II expressing cell other than the DC to maximize IL-4 responses. This ancillary role was initially attributed to the basophil (Ba) (9, 14, 15), as mAb

Corresponding Author: Michael F. Gurish, Ph.D. Phone: 617-525-1235 FAX: 617-525-1310 mgurish@partners.org.

depletion of Ba greatly inhibits Th2 polarization, but subsequent studies using Ba-deficient mice have called this finding into question (12).

In the interest of identifying a second MHC-II$^+$ cell involved in the local response to papain, we injected C57BL/6 mice in the footpad with fluorescently labeled papain and followed papain uptake in the PLN by flow cytometry. We found an unexpectedly rapid and strong uptake of papain by B cells that also occurred in transgenic MD4 mice, in which 98% of B cells express a BCR specific for hen egg lysozyme (HEL). This uptake by polyclonal B cells occurred within minutes after injection and B cells subsequently internalized papain into endosomes. These findings suggested that papain acquisition by B cells involved an innate B cell response to cysteine protease activity rather than cognate-specific uptake by the clonotypic BCR.

This prompted a study of papain immunization in B cell-deficient μMT mice (16), which showed normal PLN T cell expansion but significantly impaired peak IL-4 induction in both conventional Th2 cells and follicular helper T cells (Tfh) at d 5–6. Reconstitution of the B cell compartment in μMT mice restored papain-induced development of the Tfh and Th2 compartments. Mechanistic studies pointed to the inducible T cell costimulator (ICOS)/ICOS-Ligand (ICOS-L) pathway as central to this amplification. T cells strongly upregulated ICOS following papain immunization, peaking at d 5 post-immunization, and ICOS-L was expressed on B cells but not by DCs at this time point. T cell ICOS upregulation was partially dependent on B cells, as μMT mice showed normal increases in ICOS expression at d 3 but impaired upregulation on d 4–5 post-immunization. ICOS-L blockade with neutralizing mAb inhibited IL-4 induction in wild type (WT) mice but did not further reduce the already diminished IL-4 induction in μMT mice. Our findings reveal innate uptake of papain by B cells and suggest that the B cell is the essential MHC-II$^+$ auxiliary cell needed for a full primary Th2 response to cysteine protease immunization. The B cell acts at least partially through ICOS-L costimulation, which significantly augments DC-dependent Th2 and IL-4$^+$ Tfh induction in response to cysteine protease immunization.

Materials and Methods

Mice

7 to 12 wk old C57BL/6J, μMT (B6.129S2-*Igh-6*^{tm1Cgn}/J, STAT6$^{-/-}$ (B6.129S2(C)-*Stat6*^{tm1Gru}/J), IL4$^{-/-}$ (B6.129P2-*Il4*^{tm1Cgn}/J), and MD4 (C57BL/6-Tg(IghelMD4)4Ccg/J) mice were obtained from The Jackson Laboratory (Bar Harbor, ME, stock #000664, 002288, 005977, 002253, and 002595, respectively), and maintained in-house at the Dana Farber Cancer Institute. CD21-cre (B6.Cg-Tg(Cr2-cre)3Cgn/J) and tdTomato (B6.Cg-Gt(ROSA)$^{26Sortm14(CAG-tdTomato)Hze}$/J) mice were obtained from The Jackson Laboratory (stock #006368 and 007914, respectively) and housed at Harvard Medical School. CR2$^{-/-}$ mice were housed at Harvard Medical School as previously reported (17). All mice were housed under specific pathogen free conditions, and the use of all mice for these studies was in accordance with institutional guidelines with review and approval by the Animal Care and Use Committee of the Dana Farber Cancer Institute.

Papain administration

Fifty μl of papain diluted to a concentration of 1 mg/ml (Sigma-Aldrich, St. Louis, MO) in HBSS were injected subcutaneously into the bilateral footpads on d 0, and the mice were sacrificed for harvest of the PLN at d 5 unless otherwise noted. For fluorescently labeled papain experiments, papain was labeled with either an AF647 or AF488 labeling kit (Life Technologies, San Diego, CA) according to the manufacturer's protocols and the labeling reaction was stopped using the optional hydroxylamine hydrochloride (Sigma-Aldrich) stopping step. Following labeling, samples were dialyzed for 18 h in 4 changes of HBSS in a Slide-A-Lyzer Dialysis Cassette (Thermo Scientific, Rockford, IL). Prior to injection, any remaining unreacted dye was removed using a Micro Bio-Spin 30 chromatography column (Bio-Rad, Hercules, CA). This process yielded a degree of labeling of approximately 5 moles fluorophores per mole papain. As a control, OVA (Sigma-Aldrich, St Louis, MO)) was labeled in parallel to a similar degree of labeling. For intravital microscopy, mice were injected with 10 μl papain at a concentration of 10 mg/ml.

Flow Cytometric analysis

Fluorescently conjugated mAb directed against the following epitopes (clone) were used for flow cytometric analysis: CD3 (17A2), CD4 (RM4–5), CD19 (6D5), MHC-II (M5/114.15.2), CD11c (N418), CD11b (M1/70), IL-4 (11B11), IFN-γ (XMG1.2), FcεR1α (MAR1), CD49b (DX5), ICOS (7E.17G9), ICOS-ligand (HK5.3), CD80 (16-10A1), CD86 (GL-1), PD-1(RMP1-30), CXCR-5(L138D7). Staining with each mAb was compared to an isotype-matched control using fluorescence minus one. All mAb were purchased from Biolegend.

Single-cell suspensions of spleen and LN were obtained by grinding tissues through 70-mm cell strainers (BD Biosciences, San Diego, CA) into HBSS supplemented with 2% heat-inactivated FBS. Nonspecific mAb binding was blocked with anti-CD16/32 (2.4G2) (BD Biosciences) for 10 min, and appropriate mAb were added for 30 min. Cells were analyzed on a FACSCanto II flow cytometer (BD Biosciences) using FACSDiva acquisition software. FlowJo software (Tree Star, Ashland, OR) was used for data analysis.

To assess intracellular cytokine production by $CD4^+$ T cells, LN cells were resuspended in culture medium supplemented with 10% FBS, L-glutamine, penicillin, streptomycin, gentamicin, HEPES buffer, sodium pyruvate, and 2-mercaptoethanol (Sigma-Aldrich). PMA and Ionomycin (Fisher Scientific) were added for 2 h, after which 1 μg/mL Brefeldin-A (BD Biosciences) was added for an additional 2 h. At this point, cells were harvested, spun down, stained for extracellular markers, fixed and permeabilized using a BD Cytofix/Cytoperm kit according to the manufacturer's protocol, and stained intracellularly for cytokine production. Gating to determine positive cytokine expression was set using samples stained with an isotype control antibody such that 0.1% of isotype control stained events fell in the positive gate.

Sublethal irradiation and bone marrow (BM) reconstitution

μMT mice were irradiated with a sublethal dose of 400 rad and injected i.v. with 10^6 WT BM cells after resting for 24 h. These reconstituted mice, along with non-irradiated μMT

littermates and age-matched WT mice, were rested in the Dana Farber animal facility for 8 wks, after which they were immunized in the footpad with papain and their responses analyzed after 5 d.

Confocal Microscopy

PLN from mice immunized with AF647-labeled papain were isolated after 24 h and fixed in 4% paraformaldehyde for 4 h. Fixed PLNs were soaked in 30% sucrose overnight and then embedded in optimal cutting temperature compound for cryostat sectioning. To assess internalization of papain by follicular B cells in the PLN and ensure that only B cells were being analyzed, image sections were chosen based on the presence of B cells and the absence of immunofluorescent staining for macrophages or follicular DC. Colocalization of AF647-labeled papain with the B cell surface marker IgD and the endosomal marker EEA-1 was assessed for each captured image. PLN sections were stained with the indicated mAb and imaged using standard confocal microscopy on an Olympus Fluoview FV1000 confocal microscope. Data was acquired by Olympus Fluoview 1000 software, and basic post-capture processing (brightness/threshold adjustment) was performed in Volocity. Fluorochromes used include Pacific Blue, DyLight405, AF488, FITC, AF568, PE, AF633, and APC. Lenses – Olympus 10x NA: 0.45; 20x NA: 0.7; 60x/W NA: 1.2.

Intravital Multiphoton Microscopy

C57BL/6 mice were given 5×10^6 naïve B cells isolated from CD21-cre_tdTomato reporter mice by intravenous injection 24 h prior to imaging. Recipient mice were anesthetized with 2% isofluorane, and prepared on a surgical board for PLN live imaging. Exposed PLNs were monitored for physiological temperature maintenance, and imaged using a Zeiss-BioRad Radiance 2100 Multiphoton microscope. Data was acquired by LaserSharp 2000 software. All live imaging data was collected at 34 degrees C as assessed by a temperature probe at the exposed LN site. AF488-labeled papain was injected in the footpad at time point 0, and serial 150 micrometer (μm) depth captures (3 μm steps) were taken every 2 min for at least 60 min following papain injection. 4 dimensional data reconstruction was done using Volocity image analysis software, and subsequent 2-dimensional quantitation was processed using CellProfiler (http://www.cellprofiler.org/citations.shtml). Fluorochromes include Pacific Blue, AF488, and tdTomato. Lenses – Olympus XLUMPlanFl 20x/W NA: 0.95; Leica HC PL Fluotar 10x NA: 0.3.

mAb-mediated blockade

For inhibition of the ICOS/ICOS-L pathway, mice were injected on d 0 with 250 μg of anti-ICOS-L or the appropriate isotype control mAb (BioLegend, San Diego, CA). Mice were then injected in the footpad with papain, and cytokine production in the PLN was assessed after 5 d.

Statistical analysis

Data are expressed as the mean ± SD when derived from 3 or more values. Significance was determined with a two-tailed Student t test where 3 or more values were available for analysis. ANOVA was used to determine statistical significance for intravital microscopy

experiments and MFI changes over time. The Pearson product-moment correlation coefficient was used to analyze association of papain with IgD or EEA-1 and statistical significance was determined using a paired Student's t-test. A p value of $< 0.05\%$ was considered to be significant.

Results

The majority of papain-binding cells in the PLN within the first 24 h following footpad injection are CD19$^+$ B cells, which subsequently internalize papain

To determine which MHC-II$^+$ cells were interacting with papain following immunization, papain was labeled with the fluorophore AlexaFluor (AF) 647 and injected bilaterally into the hind footpads of mice. After 24 h, the mice were sacrificed and the draining PLN analyzed via flow cytometry. Analysis of all MHC-II$^+$ cells showed that slightly over 1% were positive for papain and, strikingly, the majority of these papain$^+$ MHC-II$^+$ cells were CD19$^+$ B cells (Fig. 1A). The remaining papain$^+$, MHC-II$^+$ cells consisted of a mixture of CD11c$^+$ and CD11c$^+$, CD11b$^+$ DC and CD11b$^+$ macrophages (data not shown). Although Ba (CD49b$^+$, FcεR1α$^+$) have been previously reported to act as APC in the papain model (9), at no point were we able to detect AF647-labeled papain being taken up by Ba in PLN (data not shown).

As this uptake of papain by B cells was both substantial and unexpected, we compared papain uptake to that of labeled OVA, using unlabeled papain as a control. A significant percentage of B cells, 1.48%, were positive for labeled papain at 24 h, while only 0.19% of B cells were positive for OVA, a non-significant increase over unlabeled controls (Fig. 1B, C). This B cell acquisition of papain could be observed as early as 1 h post-immunization, at which point B cells made up the vast majority of papain$^+$ cells in the PLN (Fig. 1D).

The B cell preference for papain uptake over OVA suggested that papain acquisition occurred in a manner not mediated by the specificity of the BCR. To confirm this, papain uptake by B cells from WT mice was compared to that of B cells from transgenic MD4 mice, of which 98% carry a BCR specific for HEL (18). MD4 mice also readily acquired papain 1 h after immunization (Fig. 1E), and no significant difference in papain uptake was observed between WT and MD4 mice (Fig. 1F). There was also no difference in papain uptake between B cells from WT mice and B cells from mice lacking complement receptor 2 (CR2), another mechanism through which B cells have been reported to acquire Ag (19) (not shown).

We next confirmed B cell acquisition of papain with confocal microscopy. AF647-labeled papain was readily observable in the B cell follicle, colocalizing with B cells in a punctate pattern suggesting the Ag might be in vesicles (Fig. 2A). To assess whether this pattern indicated internalization of papain by follicular B cells, C57BL/6 mice were injected with AF647-labeled papain in the footpad and the PLNs were harvested and fixed for imaging 24 h following injection. Initial experiments showed that AF647-labeled papain appeared to co-localize with the early endosomal marker endosomal Ag-1 (EEA-1) (20) (Fig. 2B). This was confirmed by measuring the correlation of the papain signal with EEA-1 versus a general correlation with the B cell membrane, identified using anti-IgD. This revealed a significantly

higher correlation with the endosomal marker, indicating that papain in these regions was internalized into endosomes by resident B cells (Fig. 2C). As papain uptake was not dependent on either CR2 or BCR Ag specificity, this uptake and internalization of a cysteine protease represents a novel innate mechanism of B cell uptake of an allergenic Ag.

Intravital microscopy reveals B cell uptake of papain within minutes following footpad injection

We next used multiphoton intravital microscopy to observe the *in situ* uptake of labeled papain by B cells. To mark the B cells *in vivo*, fluorescently labeled B cells from CD21-cre_tdTomato reporter mice were adoptively transferred into C57BL/6 mice, and 24 h later the mice were injected in the right footpad with AF488-labeled papain. The uptake of papain by tdTomato$^+$ B cells in the PLN was monitored every 2 min for 60 min following injection (Fig. 2D). The assayed PLN region was bathed in papain within minutes following footpad injection, suggesting Ag entry into the PLN via the conduit network. Overall papain intensity within the PLN increased over time, beginning as early as 10 min and peaking between 30 and 40 min (Fig. 2E & supplemental movie 1). At the same time there was also an increase in papain uptake by individual B cells, reaching a plateau at 40 min and remaining constant at this level for the duration of the experiment (Fig. 2F). An analysis of all tdTomato$^+$ cells determined that 60% of imaged cells were positive for papain using this technique (Fig. 2G). An in depth analysis of this response is shown in supplementary figure 1.

B cell-deficient μMT mice show no reduction in T cell expansion but markedly reduced induction of CD4$^+$, IL4$^+$ T cells in the PLN following papain immunization

Having identified a previously unreported uptake of papain by B cells, we hypothesized that there may be a role for B cells in the integrated primary PLN immune response in WT mice. Thus, we compared the PLN response in WT mice to that in B cell-deficient μMT mice, which lack mature B cells. In WT mice, both CD19$^+$ B cell and CD4$^+$ T cell expansion peaked between d 4 and 5 post-papain immunization (Fig. 3A) As PLN hypertrophy could be seen as early as several h following immunization, this peak expansion likely reflected a combination of lymphocyte recruitment and subsequent adaptive proliferation. Despite lacking B cells, μMT mice showed no reduction in CD4$^+$ T cell numbers at the d 5 peak (Fig. 3B). At d 4 post-immunization there was no difference in T cell IL-4 expression by CD4$^+$ T cells from WT mice (1.3%) and μMT mice (1.4%) (Fig. 3C). At d 5 post-immunization, CD4$^+$, IL-4$^+$ T cells increased to a mean of 3.3% in WT mice, similar to the peak levels of CD4$^+$, IL-4$^+$ T cells seen during primary responses to bee venom (21) as well as in OVA immunization using papain as an adjuvant or hookworm infection (10); representative plots from d 5 are shown (Fig. 3D). However, there was no increase in the percentage of CD4$^+$, IL-4$^+$ T cells in μMT mice between d 4 and 5, with a mean of 1.1% at d 5. At 6 d post-immunization, the percentage of CD4$^+$ T cells expressing IL-4 declined in both strains, to 2.1% in the WT and 0.61% in the μMT. Thus, while B cells did not influence CD4$^+$ T cell expansion following papain immunization, they profoundly amplified IL-4 induction in this cell population.

μMT mice show impaired papain-induced Th2 and Tfh cell induction, which is restored through B cell reconstitution

As both effector Th2 cells and Tfh cells are $CD4^+$ T cells capable of producing IL-4, we evaluated the effects of B cell deficiency on each of these compartments. Follicular helper T cells express high levels of the chemokine receptor CXCR5 and the T cell activation marker programmed cell death protein-1 (PD-1) (22) while conventional effector Th2 cells express IL-4 but lower levels of CXCR5 (23). PD-1^{hi}, $CXCR5^{hi}$ Tfh were readily detectable in both WT and μMT mice. IL-4 expression by both Tfh and effector Th2 cells could be observed in both strains, but the induction of IL-4 was reduced in both populations in the absence of B cells (Fig. 4A). The expansion of Tfh was also reduced by ~3 fold in μMT (Fig. 4B), consistent with previous reports in other models showing a B cell dependence for the expansion of Tfh cells (24). In WT mice, effector Th2 cells represented 2.3% of $CD4^+$ T cells and IL-4^+ Tfh cells represented 1% of CD4+ T cells (Fig. 4C). In the μMT strain, these $CD4^+$ T cell compartments were reduced to 0.65% for Th2 cells and only 0.14% for IL-4^+ Tfh. This represented a 3.5 fold reduction in Th2 cells and a 7-fold reduction in IL-4^+ Tfh in the absence of B cells. Thus, B cell deficiency suppressed both expansion and IL-4 induction in Th2 effector and Tfh cells.

To assess whether the B cell deficiency accounted for these findings, the B cell compartment in μMT mice was restored via sublethal irradiation followed by adoptive transfer of WT BM. After 8 wks, the B cell compartment in both the spleen and PLN was restored to near-WT levels (Fig. S2). Reconstitution of μMT mice restored papain-induced Tfh expansion (Fig. S3 A, B), Tfh IL-4 production and Th2 polarization to levels comparable to WT mice (Figure S3 A, C). Similar results were obtained using lethal irradiation of μMT mice followed by reconstitution with WT BM (not shown).

Papain immunization induces STAT-6-dependent upregulation of MHC-II and CD86 expression by PLN B Cells

Based on the finding that B cells acquire papain and are important regulators of papain-induced Th2 and Tfh responses, we evaluated MHC-II and CD86 expression on B cells as these proteins are essential to Ag presentation. MHC-II was strongly expressed on naïve B cells and steadily increased in expression between d 3 and d 5, at which point expression had increased 2.7 fold over naïve levels (Fig. 5A). CD86 expression was barely detectable on naive B cells, increased in expression on d 3–4 post-immunization and reached a peak on d 5 (Fig. 5B). In both cases this reflected increased expression on most or all B cells in the PLN. Expression of B cell activation markers peaked on the same day as the numbers of IL-4^+, $CD4^+$ T cells in WT mice.

Despite the fact that less than 2% of B cells were positive for labeled papain at 24 h (Fig. 1B) and B cells greatly expand between d 0 and d 5 (Fig. 3A), all B cells in the PLN on d 5 exhibited robust upregulation of MHC-II and CD86 (Fig. 5A, B), suggesting a soluble signal was responsible. We thus evaluated whether this B cell activation was IL-4 dependent by comparing the MHC-II and CD86 upregulation on B cells from papain immunized WT and $STAT6^{-/-}$ mice, which are unable to respond to IL-4 signaling. $STAT6^{-/-}$ mice immunized with papain showed no increase in these activation markers over naïve levels (Fig. 5C). The

same results were observed in IL-4$^{-/-}$ animals (Fig. 5D), confirming that PLN B cell MHC-II and CD86 upregulation following papain immunization is an IL-4 dependent process.

ICOS-L is expressed on B cells but not DC and ICOS is strongly upregulated on CD4$^+$ T cells at d 4–6 following papain immunization of WT Mice

Due to the observed upregulation of MHC-II and CD86 on PLN B cells, we considered whether a TCR-dependent costimulatory signal might contribute to the IL-4$^+$ T cell response. As the costimulatory ligand ICOS-L on APC and ICOS on CD4$^+$ T cells has previously been associated with CD4$^+$ IL-4 induction (25), expression of this costimulatory pair on B cells and T cells was assessed. ICOS-L was present on naïve B cells in the PLN at baseline, persisted to d 3–4 post-papain immunization and then decreased on d 5 post-immunization (Fig. 6A), suggesting an interaction with ICOS (26). ICOS-L was not expressed on PLN DC at the peak of T cell IL-4 induction (Fig. 6B). We observed a slow, steady increase in the percentage of CD4$^+$ T cells expressing ICOS between d 0 and 3 in both WT and μMT mice, with 17% of T cells expressing ICOS at this time point in both strains (Fig. 6C). Between d 4 and 5 there was a significant increase in ICOS expression on CD4$^+$ cells from WT mice such that 40% of CD4$^+$ cells in the LN were ICOS positive at d 5. This increase was significantly blunted in μMT mice, with 26% of CD4$^+$ T cells expressing ICOS at the d 5 peak. By d 6, expression began to decline in both WT and μMT mice, with WT mice maintaining higher expression than μMT animals. Unlike the uniform changes in B cell MHC-II and CD86 expression (Fig. 5), the changes in ICOS expression involved only a subset of CD4$^+$ T cells (Fig. 6D). Taken together, the impaired responses for the μMT strain imply a B cell role in the incremental T cell ICOS expression and Th2 polarization seen in WT mice.

Monoclonal antibody blockade of ICOS-L inhibits induction of Th2 and Tfh cells in WT but not μMT mice

The findings that ICOS expression and IL-4 induction on CD4$^+$ T cells peaked at d 5 at the same time that B cell MHC-II and CD86 expression peaked and ICOS-L expression declined suggested that ICOS-ICOS-L costimulation could be a mechanism through which B cells influenced papain-induced IL-4 induction. Thus, the functional importance of ICOS-L in papain-induced Th2 polarization was assessed by mAb blockade. WT and μMT mice were injected i.p. with an anti-ICOS-L neutralizing mAb or the appropriate isotype-matched control IgG on d 0 followed by subcutaneous administration of papain into the footpads and analysis of the PLN by cytometry 5 d later. In WT mice, ICOS-L blockade suppressed both the generation of Tfh and their IL-4 production (Fig. 7A, C), consistent with previous findings establishing the central role of ICOS/ICOSL interactions in the generation of Tfh (27). ICOS-L blockade also suppressed the generation of Th2 cells in WT mice (Fig. 7A, D), indicating a role for either ICOS-L or ICOS-L-responsive cells in the generation of Th2 cells. ICOS-L blockade did not further reduce the already impaired generation of Tfh and Th2 responses in μMT mice (Fig. 7B, D). While ICOS-L blockade significantly impaired both Th2 and Tfh responses, it did not reduce Tfh generation in WT mice to μMT levels (Fig. 7C), nor did it fully reduce IL-4 production by either Tfh or Th2 cells (Fig. 7D).

Discussion

We initially examined the papain footpad model because cysteine proteases are components of several common allergens, including house dust mite (2) and grass pollen (1), and there was controversy in the literature as to the involvement of a second cell ancillary to the DC in maximizing the Th2 response to papain in the PLN (9, 11, 12). Furthermore, this model allows a unique opportunity to analyze the cellular events involved in a primary Th2 response in the draining LN to a cysteine protease Ag with Th2 adjuvant activity (8, 28) through direct assays over a 6 d time period.

We began in an unbiased fashion by injecting naïve mice with fluorescently labeled papain to identify interacting cells that might drive or regulate Th2 polarization. The majority of cells taking up papain in the PLN were B cells by flow cytometric analysis and the percentage of B cells positive for papain was strikingly high compared to OVA uptake, suggesting an innate reaction to the protease activity rather than cognate-specific uptake directed by the BCR. This was confirmed through experiments with the HEL BCR transgenic mouse that revealed papain uptake was unaltered by the HEL specificity of the BCR. Furthermore, after acquiring papain the B cells internalized the Ag and directed it to endosomes. This uptake of papain was not mediated by CR2, another BCR-independent pathway through which B cells have been shown to acquire Ag (19). Intravital multiphoton microscopy highlighted that B cells proximal to the subcapsular sinus rapidly acquired papain from lymphatic flow following immunization, both confirming the flow cytometry findings and adding evidence for a direct mechanism of uptake. Thus, our initial findings recognized a novel innate mechanism through which B cells acquire a cysteine protease Ag.

Although the papain model of Th2 inflammation has been used by numerous groups over the past several years, there is uncertainty regarding the receptors and cell types driving the immune response to papain. However, the proteolytically active site of papain is required for it's immunogenicity, as both heat inactivation and treatment with a specific cysteine protease inhibitor eliminate the immune responses against papain (8). Liang et al. showed that papain can activate naïve T cells through protease activated receptor (PAR)-2 cleavage, leading to T cell production of cytokines and chemokines (29). As PAR-2 expression by B cells has also been reported (30), papain could be stimulating B cell capture and internalization through a similar mechanism. Additionally, papain's ability to cleave immunoglobulin into Fc and Fab regions has been long established (31), raising the possibility that active site interactions with non-Ag-specific regions of the BCR could lead to internalization. Additionally, other surface proteins found on the B cell such as CD23 can be cleaved by papain-family cysteine proteases such as DerP1 (32). However, it is also possible that papain endocytosis is mediated by a yet undescribed receptor.

A comparison of the cellular events leading to IL-4 induction in PLN $CD4^+$ T cells in WT and μMT mice revealed a previously undescribed role for B cells in this process. B cell-deficient mice showed significantly reduced percentages of IL-4^+, $CD4^+$ T cells in the PLN at the d 5 peak of the papain immune response but had no impairment in overall T cell expansion. This deficit in the level of IL-4^+ $CD4^+$ cells represented both a reduction in effector Th2 cell generation and in Tfh expansion and decreased induction of IL-4 in these

populations. Restoration of the B cell compartment in μMT mice restored both Th2 and Tfh responses, highlighting the important role for B cells in each compartment.

The finding that B cell upregulation of MHC-II and CD86 are both IL-4 and STAT6-dependent processes strongly suggested a role for Tfh cells in the observed B cell activation. These cells generate IL-4 *in situ* in the B cell follicle (33, 34) and this cytokine was previously described to induce upregulation of both MHC-II and CD86 on B cells (35). As the generation of both IL-4$^+$ Tfh and Th2 effector cells was impaired in the absence of B cells, B cells and Tfh play a reciprocal role in activating each other during the immune response to papain, consistent with other findings regarding the interplay between these two cells (36). This interplay is likely necessary for the simultaneous B cell amplification of Th2 polarization, as B cell activation is greatly impaired in STAT6$^{-/-}$ and IL-4$^{-/-}$ mice and B cell costimulatory enhancement of Th2 polarization likely depends on presentation of papain on MHC-II in the context of CD86 and ICOS-L.

While IL-4 is canonically required for optimal Th2 polarization, ligation of costimulatory molecules on the T cell surface can also modulate Th2 polarization. CD86 blockade during leishmania infection can inhibit pathogen-induced Th2 polarization, skewing the immune response to a Th1 phenotype and improving host clearance of the pathogen (37). ICOS ligation on naïve CD4$^+$ T cells in conjunction with a TCR signal enhances IL-4 and IL-10 production while inhibiting IL-2 production (25). CD4$^+$ cells from mice deficient in ICOS and immunized with KLH and alum show defective IL-4 production following restimulation with KLH, and the in vivo IgE and IgG1 responses in these mice are also impaired (38). Signaling through both ICOS and CD28, the ligand of CD86, is necessary for full Th2 polarization in a model of *S. mansoni* egg Ag-induced airway inflammation (39), suggesting that B-7 family members and ICOS act together to potentiate Th2 polarization. Neither the latter study nor several others examining ICOS-mediated Th2 polarization identified the source of ICOS-L expression (38, 40).

In the papain model, ICOS-L expression on B cells increased modestly but not significantly at d 3–4 before decreasing at d 5, and expression of this costimulatory receptor was not observed on DCs or any other APC in the PLN during the d 5 peak of the IL-4 response. ICOS upregulation on CD4$^+$ T cells was significantly reduced in μMT mice compared to WT mice at d 4–6 post-papain immunization, with the largest differences occurring during d 5–6, when IL-4 production was also profoundly impaired. These findings suggested a potential link between the ICOS/ICOS-L pathway and subsequent B cell-dependent IL-4 production by LN CD4$^+$ T cells. Supporting this link, administration of an ICOS-L blocking mAb reduced IL-4 production in WT mice but did not further reduce the already impaired Th2 polarization in μMT mice.

While the role of ICOS in supporting the generation of Tfh cells is well characterized (24), its role in supporting effector Th2 polarization is more controversial (41, 42). ICOS-L blockade impaired Th2 polarization in addition to suppressing Tfh responses to papain. Thus, our results support a role for this pathway in the generation of both cell types. However, ICOS-L inhibition did not fully reduce WT Th2 or Tfh responses to the levels seen in the μMT. This could indicate either incomplete inhibition of ICOS-L or point to

other pathways also playing an important role in B cell support of Th2 and Tfh responses. The magnitude of the difference in ICOS upregulation in the absence of B cells (<2 fold) was modest compared to the impact on IL-4 induction (~3 fold), further highlighting the effect of B cells on optimizing the Th2 and Tfh responses in this model. Importantly, this pathway acts subsequent to an early DC-dependent event that initiates the development of each cell type as some level of Tfh and Th2 effector cells can be seen in the absence of B cells.

While no studies thus far have posited a role for B cells in papain-induced Th2 polarization, several studies have highlighted a role for B cells in supporting Th2 polarization in parasite infection models. B cell-deficient JHD mice infected with *S. mansoni* exhibit impaired $CD4^+$ T cell IL-4 and IL-10 production accompanied by increased IFN-γ and IL-12 generation compared to WT mice, indicating a role for B cells in influencing the Th1/Th2 balance in this model (43). Furthermore, μMT mice infected with *N. brasiliensis* have greatly impaired IL-4 secretion by $CD4^+$ cells, indicating a B cell-dependent Th2 polarization in another infection model (44). The surface costimulatory receptors CD80 and CD86 are central to this B cell-dependent T cell polarization, as reconstitution of B cell-deficient mice with WT B cells restores Th2 polarization while reconstitution with CD80 and CD86 deficient B cells does not. Adoptive transfer of IL-4-deficient B cells fully reconstitutes the Th2 response, showing that B cell production of IL-4 is not a relevant mechanism (44). A role for B cells was also identified in coordinating the colocalization of $CXCR5^+$ DC and both Tfh and Th2 cells during *H. Polygyrus* infection, thereby enhancing IL-4 production by each T cell subset (23).

In summary, our results indicate that during the allergic response to papain, draining LN resident B cells rapidly acquire cysteine protease Ag directly from lymphatic flow following immunization via an innate mechanism dependent on its protease activity and subsequently internalize the Ag. They are later joined by peripheral migratory DC carrying the protease from the site of immunization. The DC plays a major early role in the LN response, likely driving the expansion of the $CD4^+$ T cell population and mediating initial IL-4 induction and expansion of B cells in the LN. These activated B cells enhance $CD4^+$ T cell ICOS expression beginning on d 4 and then amplify Th2 polarization and Tfh induction in an ICOS-L/ICOS dependent manner during d 5–6. We speculate that the B cells that acquired papain at d 0 in a noncognate manner then process and retain Ag during expansion so as to present the Ag to papain-specific T cells on d 4–5. This cognate presentation occurs in the context of MHC-II along with ICOS/ICOS-L and CD86/CD28 costimulation, thereby amplifying IL-4 production by both effector Th2 cells and Tfh. This IL-4 production by Tfh further activates B cells, increasing their expression of surface proteins associated with Ag presentation and possibly acting to enhance B cell-T cell interactions and subsequent IL-4 induction in both T cell compartments. Taken together, our findings identify a novel non-canonical mechanism through which B cells acquire a cysteine protease Ag with Th2 adjuvant activity and reveal a previously uncharacterized co-stimulatory role for B cells in T cell ICOS expression and Th2 polarization following papain immunization.

Supplementary Material

Refer to Web version on PubMed Central for supplementary material.

Acknowledgments

The authors wish to thank Dr. Peter Sage for many helpful conversations.

This work was supported by the following grants from the National Institutes of Health: P50-GM52585, R01-AI083516, P01-AI078897, R01-AI039246.

Abbreviations used in this article

Ba	basophil
BM	bone marrow
DC	Dendritic Cell
ICOS	Inducible T cell costimulator
NS	no significant difference
PD-1	programmed cell death protein 1
PLN	popliteal lymph node
Tfh	Follicular helper T cell
Th2	T helper type 2 cell

References

1. Grobe K, Becker WM, Schlaak M, Petersen A. Grass group I allergens (beta-expansins) are novel, papain-related proteinases. Eur. J. Biochem. 1999; 263:33–40. [PubMed: 10429184]
2. Chua KY, Stewart GA, Thomas WR, Simpson RJ, Dilworth RJ, Plozza TM, Turner KJ. Sequence analysis of cDNA coding for a major house dust mite allergen, Der p 1. Homology with cysteine proteases. J. Exp. Med. 1988; 167:175–182. [PubMed: 3335830]
3. Gough L, Sewell HF, Shakib F. The proteolytic activity of the major dust mite allergen Der p 1 enhances the IgE antibody response to a bystander antigen. Clin. Exp. Allergy. 2001; 31:1594–1598. [PubMed: 11678860]
4. Finkelman FD, Madden KB, Cheever AW, Katona IM, Morris SC, Gately MK, Hubbard BR, Gause WC, Urban JF Jr. Effects of interleukin 12 on immune responses and host protection in mice infected with intestinal nematode parasites. J. Exp. Med. 1994; 179:1563–1572. [PubMed: 7909327]
5. McKerrow JH, Caffrey C, Kelly B, Loke P, Sajid M. Proteases in parasitic diseases. Annu. Rev. Pathol. 2006; 1:497–536. [PubMed: 18039124]
6. Robinson MW, Dalton JP, Donnelly S. Helminth pathogen cathepsin proteases: it's a family affair. Trends Biochem. Sci. 2008; 33:601–608. [PubMed: 18848453]
7. Simpson RJ, Nice EC, Moritz RL, Stewart GA. Structural studies on the allergen Der p1 from the house dust mite Dermatophagoides pteronyssinus: similarity with cysteine proteinases. Protein Seq. Data Anal. 1989; 2:17–21. [PubMed: 2911558]
8. Sokol CL, Barton GM, Farr AG, Medzhitov R. A mechanism for the initiation of allergen-induced T helper type 2 responses. Nat. Immunol. 2008; 9:310–318. [PubMed: 18300366]

9. Sokol CL, Chu NQ, Yu S, Nish SA, Laufer TM, Medzhitov R. Basophils function as antigen-presenting cells for an allergen-induced T helper type 2 response. Nat. Immunol. 2009; 10:713–720. [PubMed: 19465907]

10. Kumamoto Y, Linehan M, Weinstein JS, Laidlaw BJ, Craft JE, Iwasaki A. CD301b dermal dendritic cells drive T helper 2 cell-mediated immunity. Immunity. 2013; 39:733–743. [PubMed: 24076051]

11. Tang H, Cao W, Kasturi SP, Ravindran R, Nakaya HI, Kundu K, Murthy N, Kepler TB, Malissen B, Pulendran B. The T helper type 2 response to cysteine proteases requires dendritic cell-basophil cooperation via ROS-mediated signaling. Nat. Immunol. 2010; 11:608–617. [PubMed: 20495560]

12. Ohnmacht C, Schwartz C, Panzer M, Schiedewitz I, Naumann R, Voehringer D. Basophils orchestrate chronic allergic dermatitis and protective immunity against helminths. Immunity. 2010; 33:364–374. [PubMed: 20817571]

13. Gao Y, Nish SA, Jiang R, Hou L, Licona-Limon P, Weinstein JS, Zhao H, Medzhitov R. Control of T Helper 2 Responses by Transcription Factor IRF4-Dependent Dendritic Cells. Immunity. 2013; 39:722–732. [PubMed: 24076050]

14. Perrigoue JG, Saenz SA, Siracusa MC, Allenspach EJ, Taylor BC, Giacomin PR, Nair MG, Du Y, Zaph C, van Rooijen N, Comeau MR, Pearce EJ, Laufer TM, Artis D. MHC class II-dependent basophil-CD4+ T cell interactions promote T(H)2 cytokine-dependent immunity. Nat, Immunol. 2009; 10:697–705. [PubMed: 19465906]

15. Yoshimoto T, Yasuda K, Tanaka H, Nakahira M, Imai Y, Fujimori Y, Nakanishi K. Basophils contribute to T(H)2-IgE responses in vivo via IL-4 production and presentation of peptide-MHC class II complexes to CD4+ T cells. Nat, Immunol. 2009; 10:706–712. [PubMed: 19465908]

16. Kitamura D, Roes J, Kuhn R, Rajewsky K. A B cell-deficient mouse by targeted disruption of the membrane exon of the immunoglobulin mu chain gene. Nature. 1991; 350:423–426. [PubMed: 1901381]

17. Gommerman JL, Oh DY, Zhou X, Tedder TF, Maurer M, Galli SJ, Carroll MC. A role for CD21/CD35 and CD19 in responses to acute septic peritonitis: a potential mechanism for mast cell activation. J. Immunol. 2000; 165:6915–5921. [PubMed: 11120817]

18. Silveira PA, Dombrowsky J, Johnson E, Chapman HD, Nemazee D, Serreze DV. B cell selection defects underlie the development of diabetogenic APCs in nonobese diabetic mice. J. Immunol. 2004; 172:5086–5094. [PubMed: 15067092]

19. Phan TG, Grigorova I, Okada T, Cyster JG. Subcapsular encounter and complement-dependent transport of immune complexes by lymph node B cells. Nat. Immunol. 2007; 8:992–1000. [PubMed: 17660822]

20. Mu FT, Callaghan JM, Steele-Mortimer O, Stenmark H, Parton RG, Campbell PL, McCluskey J, Yeo JP, Tock EP, Toh BH. EEA1, an early endosome-associated protein. EEA1 is a conserved alpha-helical peripheral membrane protein flanked by cysteine “fingers” and contains a calmodulin-binding IQ motif. J. Biol. Chem. 1995; 270:13503–13511. [PubMed: 7768953]

21. Palm NW, Rosenstein RK, Yu S, Schenten DD, Florsheim E, Medzhitov R. Bee venom phospholipase A2 induces a primary type 2 response that is dependent on the receptor ST2 and confers protective immunity. Immunity. 2013; 39:976–985. [PubMed: 24210353]

22. Haynes NM, Allen CD, Lesley R, Ansel KM, Killeen N, Cyster JG. Role of CXCR5 and CCR7 in follicular Th cell positioning and appearance of a programmed cell death gene-1high germinal center-associated subpopulation. J. Immunol. 2007; 179:5099–5108. [PubMed: 17911595]

23. Leon B, Ballesteros-Tato A, Browning JL, Dunn R, Randall TD, Lund FE. Regulation of T(H)2 development by CXCR5+ dendritic cells and lymphotoxin-expressing B cells. Nat. Immunol. 2012; 13:681–690. [PubMed: 22634865]

24. Choi YS, Kageyama R, Eto D, Escobar TC, Johnston RJ, Monticelli L, Lao C, Crotty S. ICOS receptor instructs T follicular helper cell versus effector cell differentiation via induction of the transcriptional repressor Bcl6. Immunity. 2011; 34:932–946. [PubMed: 21636296]

25. McAdam AJ, Chang TT, Lumelsky AE, Greenfield EA, Boussiotis VA, Duke-Cohan JS, Chernova T, Malenkovich N, Jabs C, Kuchroo VK, Ling V, Collins M, Sharpe AH, Freeman GJ. Mouse inducible costimulatory molecule (ICOS) expression is enhanced by CD28 costimulation and

regulates differentiation of CD4+ T cells. J. Immunol. 2000; 165:5035–5040. [PubMed: 11046032]

26. Logue EC, Bakkour S, Murphy MM, Nolla H, Sha WC. ICOSinduced B7h shedding on B cells is inhibited by TLR7/8 and TLR9. J. Immunol. 2006; 177:2356–2364. [PubMed: 16887997]
27. Nurieva RI, Chung Y, Hwang D, Yang XO, Kang HS, Ma L, Wang YH, Watowich SS, Jetten AM, Tian Q, Dong C. Generation of T follicular helper cells is mediated by interleukin-21 but independent of T helper 1, 2, or 17 cell lineages. Immunity. 2008; 29:138–149. [PubMed: 18599325]
28. Pulendran B, Artis D. New paradigms in type 2 immunity. Science. 2012; 337:431–435. [PubMed: 22837519]
29. Liang G, Barker T, Xie Z, Charles N, Rivera J, Druey KM. Naive T cells sense the cysteine protease allergen papain through protease-activated receptor 2 and propel TH2 immunity. J. Allergy Clin. Immunol. 2012; 129:1377–1386. e1313. [PubMed: 22460072]
30. Busso N, Frasnelli M, Feifel R, Cenni B, Steinhoff M, Hamilton J, So A. Evaluation of protease-activated receptor 2 in murine models of arthritis. Arthritis Rheum. 2007; 56:101–107. [PubMed: 17195212]
31. Porter RR. The formation of a specific inhibitor by hydrolysis of rabbit antiovalbumin. Biochem J. 1950; 46:479–484. [PubMed: 15420176]
32. Schulz O, Sutton BJ, Beavil RL, Shi J, Sewell HF, Gould HJ, Laing P, Shakib F. Cleavage of the low-affinity receptor for human IgE (CD23) by a mite cysteine protease: nature of the cleaved fragment in relation to the structure and function of CD23. Eur. J. Immunol. 1997; 27:584–588. [PubMed: 9079796]
33. Liang HE, Reinhardt RL, Bando JK, Sullivan BM, Ho IC, Locksley RM. Divergent expression patterns of IL-4 and IL-13 define unique functions in allergic immunity. Nat. Immunol. 2012; 13:58–66. [PubMed: 22138715]
34. King IL, Mohrs M. IL-4-producing CD4+ T cells in reactive lymph nodes during helminth infection are T follicular helper cells. J. Exp. Med. 2009; 206:1001–1007. [PubMed: 19380638]
35. Marshall-Clarke S, Tasker L, Heaton MP, Parkhouse RM. A differential requirement for phosphoinositide 3-kinase reveals two pathways for inducible upregulation of major histocompatibility complex class II molecules and CD86 expression by murine B lymphocytes. Immunology. 2003; 109:102–108. [PubMed: 12709023]
36. Nutt SL, Tarlinton DM. Germinal center B and follicular helper T cells: siblings, cousins or just good friends? Nat. Immunol. 2011; 12:472–477. [PubMed: 21739669]
37. Brown JA, Titus RG, Nabavi N, Glimcher LH. Blockade of CD86 ameliorates Leishmania major infection by down-regulating the Th2 response. J. Infect. Dis. 1996; 174:1303–1308. [PubMed: 8940222]
38. Dong C, Juedes AE, Temann UA, Shresta S, Allison JP, Ruddle NH, Flavell RA. ICOS co-stimulatory receptor is essential for T-cell activation and function. Nature. 2001; 409:97–101. [PubMed: 11343121]
39. Shilling RA, Clay BS, Tesciuba AG, Berry EL, Lu T, Moore TV, Bandukwala HS, Tong J, Weinstock JV, Flavell RA, Horan T, Yoshinaga SK, Welcher AA, Cannon JL, Sperling AI. CD28 and ICOS play complementary non-overlapping roles in the development of Th2 immunity in vivo. Cell. Immunol. 2009; 259:177–184. [PubMed: 19646680]
40. Tafuri A, Shahinian A, Bladt F, Yoshinaga SK, Jordana M, Wakeham A, Boucher LM, Bouchard D, Chan VS, Duncan G, Odermatt B, Ho A, Itie A, Horan T, Whoriskey JS, Pawson T, Penninger JM, Ohashi PS, Mak TW. ICOS is essential for effective T-helper-cell responses. Nature. 2001; 409:105–109. [PubMed: 11343123]
41. Watanabe M, Watanabe S, Hara Y, Harada Y, Kubo M, Tanabe K, Toma H, Abe R. ICOS-mediated costimulation on Th2 differentiation is achieved by the enhancement of IL-4 receptor-mediated signaling. J. Immunol. 2005; 174:1989–1996. [PubMed: 15699127]
42. Tesciuba AG, Subudhi S, Rother RP, Faas SJ, Frantz AM, Elliot D, Weinstock J, Matis LA, Bluestone JA, Sperling AI. Inducible costimulator regulates Th2-mediated inflammation, but not Th2 differentiation, in a model of allergic airway disease. J. Immunol. 2001; 167:1996–2003. [PubMed: 11489981]

43. Hernandez HJ, Wang Y, Stadecker MJ. In infection with Schistosoma mansoni, B cells are required for T helper type 2 cell responses but not for granuloma formation. J. Immunol. 1997; 158:4832–4837. [PubMed: 9144498]

44. Liu Q, Liu Z, Rozo CT, Hamed HA, Alem F, Urban JF Jr. Gause WC. The role of B cells in the development of CD4 effector T cells during a polarized Th2 immune response. J. Immunol. 2007; 179:3821–3830. [PubMed: 17785819]

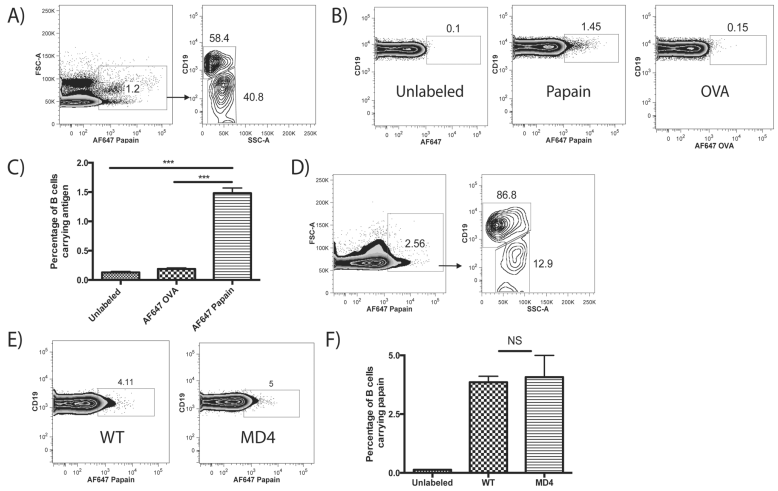

FIGURE 1.

CD19$^+$ B cells are the major Ag-bearing cell type in the PLN 24 h after footpad injection of papain and acquire papain in a non-BCR mediated manner. **(A)** Representative FACS plots of mice injected in the footpad with 50 μg AF647-labeled papain and sacrificed after 24 h. After gating on MHC-II$^+$ cells, cells positive for papain (left panel) were phenotyped, showing that CD19$^+$ cells constituted the majority of AF647$^+$ cells at 24 h (right panel). **(B)** Representative FACS plots of CD19$^+$ B cells from WT mice 24 h after injection with unlabeled papain, AF647-labeled papain, or AF647-labeled OVA. **(C)** Quantification of percentages of B cells binding AF647-labeled Ag compared to unlabeled papain controls as described in B. Bars indicate mean ± SD obtained from 2 experiments with n=3 mice per group experiment, *** indicates $p<0.001$. **(D)** Representative FACS plots of PLN cells from WT mice injected with AF647-labeled papain as described in (A) and analyzed after 1 h. **(E)** Representative FACS plots of B cells from WT and MD4 transgenic mice 1 h after injection with AF647-labeled papain. **(F)** Quantification of the percentages of WT and MD4 B cells acquiring AF647-labeled papain as described in (E). Bars indicate mean ± SD obtained from 2 experiments with n=3 mice per group per experiment, NS indicates no significant difference.

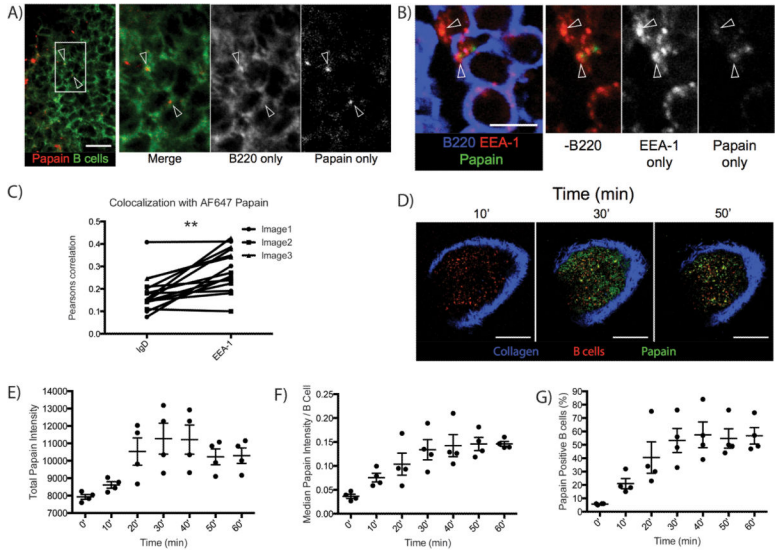

FIGURE 2.

Confocal and intravital microscopy reveal that PLN B cells rapidly acquire and subsequently internalize papain after footpad immunization. **(A)** Confocal microscopy indicating colocalization of B cells and AF647-labeled papain at 24 h post-immunization. Green indicates B220, red indicates AF647-labeled papain. Arrows indicate points of colocalization between B220 and AF647-papain. White bar indicates 14 μm. **(B)** Confocal microscopy showing colocalization of AF647-papain and the early endosomal marker EEA-1 in B cells 24 h post-immunization. Blue indicates B220, green indicates AF647-papain, and red indicates EEA-1. Arrows indicate colocalization between EEA-1 and AF647-papain on $B220^+$ B cells, and white bar indicates 5 μm. **(C)** A comparison of the Pearson correlation coefficients between AF647-labeled papain and the B cell surface marker IgD versus the early endosomal marker EEA-1. Dots indicate individual replicates and lines indicate paired observations from the same image. ** indicates $p<0.01$. **(D)** Representative images at a depth of 30 μm taken from a time course of AF647 uptake by adoptively transferred CD21-cre_tdTomato B cells in PLN of C57BL/6 mice captured at the indicated time points. AF488-papain was injected into the footpad and the PLNs were live-imaged using intravital-multiphoton microscopy. Blue indicates collagen, green indicates papain, and red indicates B cells. White bar indicates 100 μm. **(E)** Time course of total papain intensity in the PLN expressed as median of 4 depths captured as described in (D). Line and error bars indicate mean ± SD, ANOVA $p<0.001$. **(F)** Time course of median papain intensity of CD21-cre_tdTomato cells from the images in (D). Line and error bars indicate mean ± SD, ANOVA $p<0.0005$. **(G)** Time course indicating the percentage of $CD21^+$ cells identified as described in (F) positive for papain. Line and error bars indicate mean ± SD, ANOVA $p<0.0005$.

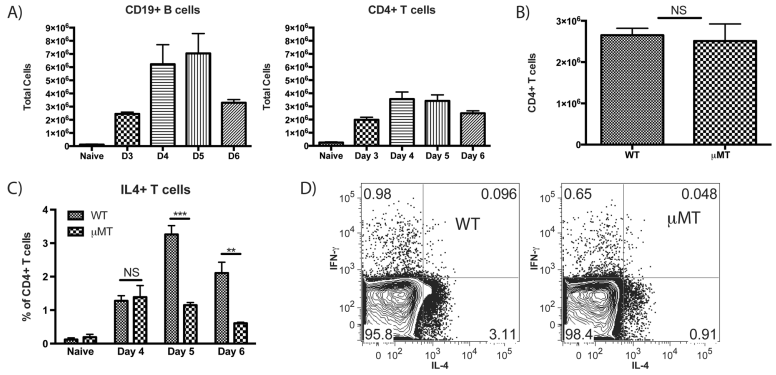

FIGURE 3.

B cell deficient µMT mice show no difference in papain-induced T cell expansion but have a marked reduction in $CD4^+$ T cell IL-4 production. **(A)** Total number of $CD19^+$ B cells and $CD4^+$ T cells in the PLN from naïve mice or papain immunized WT mice 3–6 d post-immunization. Bars indicate mean ± SD from 2–3 independent experiments per time point with n=3 mice per group per experiment. **(B)** Comparison of $CD4^+$ T cell numbers in the PLN at d 5 following papain immunization in WT and µMT mice. Bars indicate mean ± SD from 3 independent experiments with n=3 mice per group. **(C)** Time course showing the percentage of IL-4 expressing PLN $CD4^+$ T cells from naive and papain-injected WT and µMT mice at d 4–6 following papain immunization. Bars indicate mean ± SD from 2–4 independent experiments per time point with n=3–4 mice per group per experiment, NS indicates no significant difference, ** indicates $p<0.01$, *** indicates $p<0.001$. **(D)** Representative plots showing the percentages of IL-4 and IFN-γ expressing $CD4^+$ T cells from WT and µMT mice 5 d after papain immunization.

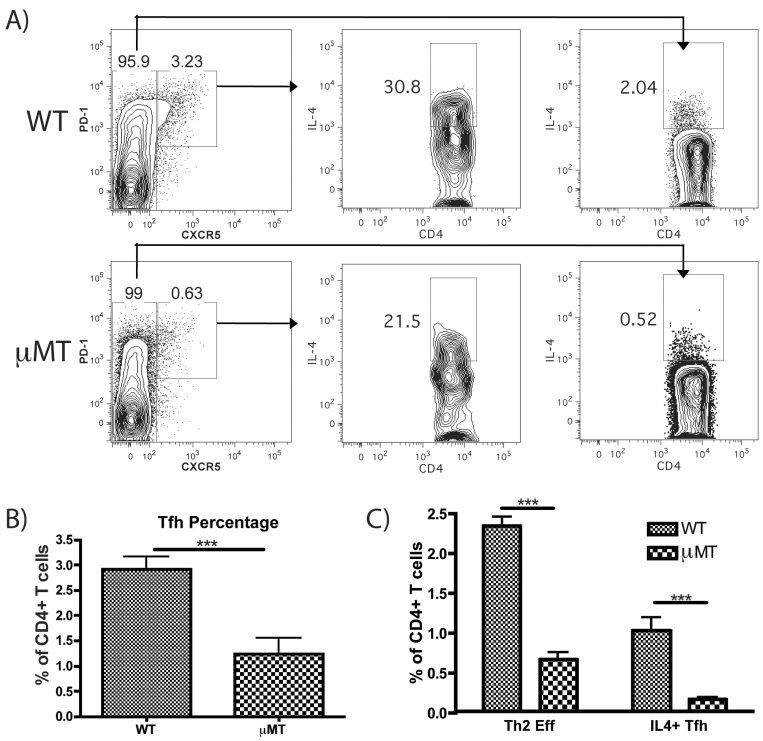

FIGURE 4.

μMT mice show impaired Tfh generation and reduced IL-4 induction by both Th2 and Tfh cells. **(A)** Representative FACS plots showing the induction of Tfh ($PD1^{hi}$, $CXCR5^{hi}$) and IL-4 expression by Tfh and conventional T cells ($CXCR5^{lo}$) in WT and μMT mice immunized in the footpad with papain 5 d earlier. **(B)** Quantification of total Tfh as a percentage of all $CD4^+$ T cells in WT and μMT mice on d 5 post-papain immunization. Bars indicates mean ± SD from 2 independent experiments with n=3 mice per group per experiment, *** indicates $p<0.001$. **(C)** Comparison of effector Th2 cells ($IL\text{-}4^+$, CXCR5 low) versus $IL\text{-}4^+$ Tfh cells ($CXCR5^{hi}$, $PD\text{-}1^{hi}$, $IL\text{-}4^+$) as a mean percentage of all $CD4^+$ T cells in WT and μMT mice 5 d post-immunization, calculated by multiplying the percentage of $CD4^+$ T cells represented by $CD4^+$ effector or Tfh cells (left panels in A) by the fraction of each population expressing IL-4 (center and right panels in A). Bars indicate mean ± SD from 2 independent experiments with n=3 mice per group per experiment, *** indicates $p<0.001$.

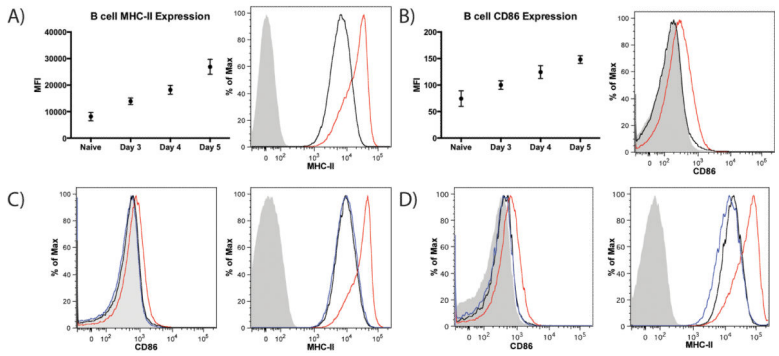

FIGURE 5.

Papain immunization increases expression of MHC-II and CD86 on PLN B cells in a STAT6 and IL-4 dependent manner. **(A)** Time course of B cell MHC-II MFI in naïve mice and in papain immunized mice 3–5 d post-papain immunization and representative histogram showing B cell MHC-II expression in naïve animals (black) and in mice immunized with papain 5 d prior (red) compared to isotype control staining (grey). Points indicate mean ± SD and data was obtained from 2 independent experiments with n=3 mice per group per experiment, ANOVA $p<0.0001$. **(B)** Time course of B cell CD86 MFI in naïve mice and in mice at d 3–5 post-papain immunization and representative histogram showing B cell CD86 expression in naïve animals (black) and in mice immunized with papain 5 d prior (red) compared to isotype control staining (grey). Points indicate mean ± SD and data was obtained from 2 independent experiments with n=3 mice per group per experiment, ANOVA $p=0.0001$. **(C)** Representative histograms indicating B cell expression of CD86 (left panel) and MHC-II (right panel) in naïve animals (black) and in WT (red) and $STAT6^{-/-}$ (blue) mice 5 d post-papain immunization compared to isotype control staining (grey). **(D)** Representative histograms indicating B cell expression of CD86 (left panel) and MHC-II (right panel) in naïve animals (black) and in WT (red) and IL-$4^{-/-}$ (blue) mice 5 d post-papain immunization compared to isotype control staining (grey).

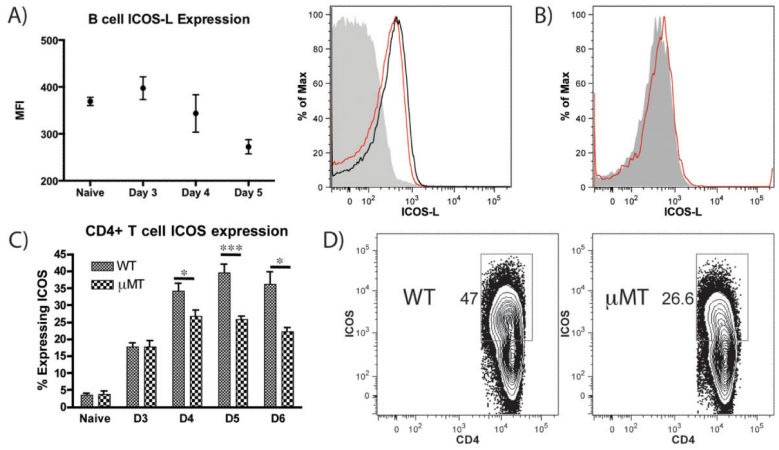

FIGURE 6.

PLN B cells express ICOS-L and µMT mice show impaired ICOS upregulation on PLN CD4$^+$ T cell after papain immunization. **(A)** Time course of B cell ICOS-L MFI in the PLN of naïve mice and papain-immunized mice 3–5 d post-immunization and representative histogram indicating B cell ICOS-L expression in naïve animals (black) and in mice immunization with papain 5 d prior (red) compared to isotype control staining (grey). Points indicate mean ± SD from 2 independent experiments, n=3 mice per group per experiment. ANOVA $p<0.05$. **(B)** Representative histogram indicating ICOS-L expression on MHC-II$^+$ CD11c$^+$ DC in mice immunized with papain 5 d previously. Red indicates ICOS-L staining and grey indicates isotype control. **(C)** Time course showing the percentage of ICOS-expressing PLN CD4$^+$ T cells in WT and µMT mice 3–6 d following papain immunization. Bars indicate mean ± SD from 2–3 experiments per time point with n=3 mice per group per experiment. * indicates $p<0.05$, *** indicates $p<0.001$ **(D)** Representative FACS plots of CD4$^+$ T cell ICOS expression in WT and µMT animals 5 d post-immunization, indicating that ICOS upregulation occurs in a subset of T cells.

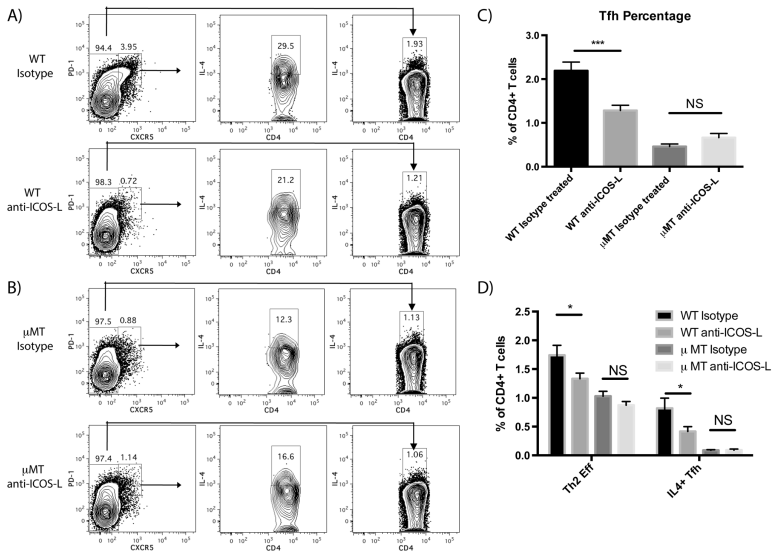

FIGURE 7.

mAb blockade of ICOS-L markedly reduces Tfh expansion and IL-4 production by Th2 and Tfh cells following papain immunization in WT but not in μMT mice 5 d post-immunization. **(A)** Representative FACS plots showing the induction of Tfh cells ($PD1^{hi}$, $CXCR5^{hi}$) and IL-4 expression 5 d post-papain immunization by Tfh and conventional $CD4^+$ T cells ($CXCR5^{lo}$) in WT mice injected i.p. with either isotype control antibody or anti-ICOS-L mAB on d 0. **(B)** Representative FACS plots showing the induction of Tfh and IL-4 expression 5 d post-papain immunization by Tfh and conventional T cells in μMT mice injected i.p. with either isotype control antibody or anti-ICOS-L mAb on d 0. **(C)** Quantification of total Tfh as a percentage of all $CD4^+$ T cells 5 d post-papain immunization in WT and μMT mice injected with either isotype control antibody or anti-ICOS-L. Bars indicate mean ± SD of n=2–3 independent experiments with 3–4 mice per experiment, *** indicates $P<0.001$, NS indicates no significant difference. **(D)** Comparison of effector Th2 cells ($IL\text{-}4^+$, $CXCR5^{lo}$) vs $IL\text{-}4^+$ Tfh cells ($CXCR5^{hi}$, $PD\text{-}1^{hi}$, $IL\text{-}4^+$) as a mean percentage of all $CD4^+$ T cells 5 d post-papain immunization in WT mice injected with either isotype control antibody or anti-ICOS-L. Bars indicate mean ± SD of n=2–3 independent experiments with 3–4 mice per experiment, * indicates $P<0.05$.